AEÜ International Journal of Electronics and Communications

Receiver Modeling for Optically Amplified Communication Systems

Ivan B. Djordjevic and Bane V. Vasic

Abstract: In this paper we determine the exact direct detection receiver decision statistics independent of optical and electrical filter choice, pulse shape and on modulation scheme, propose an advanced receiver model for the optically amplified communication system and a novel multipath interference (MPI) model independent of MPI crosstalk level, modulation format, optical and electrical filter choice as well.
The channel is modeled as a stationary additive noise channel with intersymbol interference (ISI). The additive noise composed of the amplifier spontaneous emission, multi-path interference and other additive noise sources can have arbitrary statistics. The validity of the proposed receiver model is verified by Monte Carlo simulations for different modulation schemes such as non return to zero (NRZ), return to zero (RZ), chirped return to zero (CRZ) and carrier suppressed return to zero (CSRZ) in the presence of amplifier spontaneous emission (ASE) noise, MPI and ISI. An excellent agreement is obtained for the all considered schemes.

Keywords: Optically amplified communication systems, Direct detection receiver statistics, Direct detection receiver modeling, Multi-path interference modeling

1. Introduction

Additive white Gaussian noise (AWGN) is commonly used to describe the amplifier spontaneous emission (ASE) noise [1–4], [9]. In contrast to terrestrial communication links, a typical undersea fiber communications system operates at a signal power below 0 dBm (even less than −3 dBm) per channel for N × 10 Gb/s systems, with relatively short amplifiers spacing (less then 45 km) and properly chosen dispersion compensated fiber pairs to minimize the influence of the fiber nonlinearities and dispersion [1]. The validity of the AWGN fiber channel model in considering ASE noise was confirmed for such applications through experiments [1]. However, in most terrestrial optical communication systems the AWGN assumption is not completely accurate. For example in terrestrial long-haul wavelength division multiplexing (WDM) systems, due to the interaction of fiber nonlinearities and dispersion, the WDM carriers can act as a set of pumps, and the amplifier spontaneous emission (ASE) noise spectral components can be selectively amplified. In other words the noise enhancement is much higher in certain spectral regions. This gain introduced by these effects is known as a parametric gain [4]. In this case the ASE noise is neither white nor Gaussian. Moreover, an optical filter colors the white (ASE) noise in every amplifier stage, even in the absence of parametric gain. Apart from ASE noise, in long-haul communication systems, especially those with Raman amplifiers, multipath interference (MPI) becomes an important factor in performance degradation. In an all-Raman amplifier based long-haul communications MPI is even more important factor in performance degradation. Therefore, in order to characterize the receiver performance and to design an optimal receiver it is of great importance to determine the statistics of samples at the input of the decision device.

In this paper we tackle the problem of determining such statistics in the presence of colored Gaussian noise at the receiver input and in the presence of intersymbol interference (ISI) caused by filtering.

A number of models were proposed recently [2–4]. Unfortunately, all these models lack generality. They are either restricted to a specific modulation scheme or applicable to a narrow class of optical/electrical filters. Some of them do not even consider the influence of optical filter [9]. Although the formal procedure for finding the decision statistics is well-known [3–4], [6] the probability density function (PDF) of decision statistics has been determined only a rectangular/Lorentzian optical filter transfer function and for integrate-and-dump electrical filter [3].

We propose a universal method to determine the decision statistics independent of the optical and electrical filter choice, the pulse shape or modulation scheme. The ASE noise is modeled as a Gaussian stationary colored noise with a zero-mean and known autocorrelation function. The model also takes into account the intersymbol interference. The proposed method is also applicable to other types of additive noises that accompany the ASE noise, such as multi-path interference. To compare the proposed method for finding PDF with frequently used Gaussian approximation of decision statistics, we use the skewness and the kurtosis coefficients, defined in [7–8]. The proposed method is illustrated for the case when the optical filter is modeled as a super-Gaussian filter and the electrical filter is modeled as

Received August 23, 2002. Revised April 16, 2003

Ivan B. Djordjevic, University of Bristol, Department of Electrical and Electronic Engineering, Optical Communications Research Group, University Walk, Queen's Building, Room 2.19a, Bristol, BS8 1TR, UK. E-mail: Ivan.Djordjevic@bristol.ac.uk
Bane V. Vasic, University of Arizona, Department of Electrical and Computer Engineering, 1230 East Speedway Boulevard, Tucson, AZ 85721, USA. E-mail: vasic@ece.arizona.edu
Correspondence to: I. B. Djordjevic.

1434-8411/03/57/06-381 $15.00/0

a Gaussian filter. In this case the PDF of decision statistics can be determined in a closed form. Finding an accurate receiver model is a difficult problem due to the inherent complexity of the physical phenomena involved in transmission of a digital signal and a variety of optical technologies and modulation schemes presently under investigation.

Recently several receiver models have been proposed [2], [10–14]. In the model presented in [10], the optical filter is omitted, limiting its application to NRZ/RZ signals for a very narrow region of electrical filter bandwidths. Moreover, the derivation of the signal-independent variance term assumes a flat electrical filter transfer function. In [2], [13–14], a more comprehensive model is proposed. This model, however, lacks generality since it is applicable under the white Gaussian noise approximation of the optical filter input noise, despite the fact that the ASE noise is a narrow band process. Also the analysis is restricted to NRZ receivers and MPI is ignored. The most comprehensive receiver model to date is proposed in [12]. But it is applicable for a simple integrate-and-dump type of the electrical filter for the NRZ signals. Construction of a general model, derived without any constraints with respect to either the choice of the front-end filters and modulation scheme is still an open problem.

This paper introduces a more general model, independent on the modulation scheme, pulse shape, optical and electrical filter types. It can be used for arbitrary additive stationary noise including amplifier spontaneous emission (ASE) and multipath interference (MPI). Such a model allows a comparison among different modulation schemes and in identifying the optimum filter bandwidths. Due to the generality with respect to optical and electrical filter choice, this model allows to find the optimal optical/electrical filter pair with respect to performance of every particular system. Besides the ASE noise, this model allows other types of noise, such as MPI for Raman amplifiers, without adjusting the model. The model is validated by Monte Carlo simulations. The analysis includes optically amplified CRZ, CSRZ, RZ and NRZ signals, super Gaussian optical filter and Gaussian electrical filter in the presence of ASE noise and under ISI influence.

All-Raman and hybrid Raman/erbium-doped fiber amplifiers are enabling promising technologies for dense wavelength-division-multiplexing systems [15–16]. In long-haul communication systems, especially those with all-Raman amplifiers, multipath interference [5], [17–21] is an important factor in performance degradation. Although the problem of the evolution of MPI has already been solved the problem of properly including it in Q-factor calculation is still an open issue. A number of models have been proposed so far [5], [17–21]. These models are more or less the improvement, or just implementation, of the Gaussian crosstalk model proposed in [20]. This model gives satisfying results, as will be shown latter in the text, when the MPI crosstalk power is much smaller than the observed channel power devided by the two times Q-factor squared.

We propose a novel MPI model that is independent on the MPI crosstalk level, modulation format, optical and electrical filter choice. Model includes the influence of the optical and electrical filter transfer functions as well as intersymbol interference (ISI). Due to the fact that double Rayleigh-back scattering, which is a main source of MPI, occurs in an optical fiber due to small inhomogeneities or microscopic variations in the refractive index, that reflections may occur on splices and poor connectors [5] and the fact that these sources are independent of each other, MPI can be modeled as a stationary process with an autocorrelation function determined from the measured power spectral density (PSD) function.

The paper is organized as follows. In Section 2 the exact expression for probability density function at decision circuit is derived and comparison with widely used Gaussian approximation is given. It is shown that the exact decision statistic is quite far from Gaussian. Moreover, the noise process at decision circuit is not even more stationary after the photodetection. In Section 3 we propose a simple direct detection receiver model, derived without any simplification, which takes non-stationarity of the noise process (after photodetection) into account. Finally, in Section 4 we propose a novel MPI model that allows our model proposed in Section 3 be universal and applicable to any optically amplified system, such as EDFA, all-Raman or hybrid Raman/EDFA based systems. Section 5 remained for conclusions.

2. Direct detection receiver statistics

2.1 Probability density function derivation

A typical direct detection receiver, which follows an amplifier chain, consists of a polarization filter, an optical filter, a photodiode, an electrical filter, a sampler and a decision circuit, as shown in Figure 1.

The electrical field in the fiber at the optical filter input can be written as

$$r(t) = s(t) + n(t),\ s(t) = \sum_{n=-\infty}^{\infty} \sqrt{b_n P}\, p_n(t - nT_b), \quad (1)$$

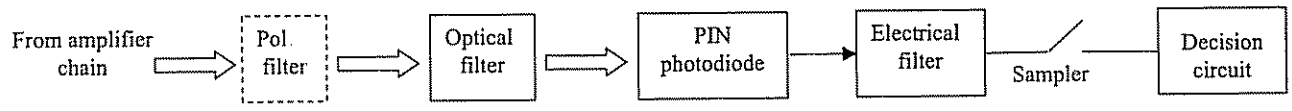

Fig. 1. Block scheme of receiver following an amplifier chain

where $s(t)$ is the ouput of the chain of (optical) amplifiers, $p_n(t)$ is the n^{th} bit pulse shape, P the peak power, and b_n is the user symbol $b_n \in \{r, 1\}$, with r being the extintion ratio, $0 \leq r < 1$. The additive noise component $n(t)$ is assumed to be a wide sense stationary (ASE, MPI, etc.) with the autocorrelation function $R_n(\tau)$. For example, in the case of ASE noise, the expression of the auto correlation function is $R_n(\tau) = N_0 R_{\text{EDFA}}(\tau)$, where $R_{\text{EDFA}}(\tau)$ is the EDFA output optical filter autocorrelation function, and N_0 is the power spectral density of ASE noise per polarization, i.e. $N_0 \simeq n_{sp}(G-1)hfN_{amp}$ (within the bandwidth of optical filter in EDFA), with n_{sp} being the spontaneous emission factor, G is an EDFA gain, hf is a photon energy, and N_{amp} is a number of amplifiers. $r(t)$, $s(t)$ and $p_n(t)$ are in fact the complex envelopes of corresponding analytical signals [3–4], [6].

Let $h_1(t)$ and $h_2(t)$ be optical filter and electrical filter impulse responses, respectively. $h_2(t)$ can be considered as the impulse response of whole receiver electronics, while $h_1(t)$, as an inverse Fourier transform of the demultiplexer (e.g., the AWG) transfer function of the observed channel. Since the optical filter is a linear susbsystem, there is no interaction between signal and noise, and both optical filter output signal $S(t)$ and noise $N(t)$ can be written as a convolution of the impulse response and corresponding filter input, that is

$$S(t) = \int_{-\infty}^{\infty} h_1(\tau)s(t-\tau)d\tau,$$
$$N(t) = \int_{-\infty}^{\infty} h_1(\tau)n(t-\tau)d\tau. \tag{2}$$

The electrical filter output $I(t)$ is a convolution of the photodiode current $i(t)$

$$i(t) = |S(t) + N(t)|^2 \tag{3}$$

and the electrical filter impulse response $h_2(t)$

$$\begin{aligned} I(t) &= \int_{-\infty}^{\infty} h_2(\tau)|S(t-\tau) + N(t-\tau)|^2 d\tau \\ &= \int_{-\infty}^{\infty}\int_{-\infty}^{\infty} K(u, v)[s(t-u) + n(t-u)] \\ &\quad [s^*(t-v) + n^*(t-v)]dudv \end{aligned} \tag{4}$$

(Photodiode responsivity is omitted without loss of generality).

$$K(u, v) = \int_{-\infty}^{\infty} h_1(u-\tau)h_2(\tau)h_1^*(v-\tau)d\tau \tag{5}$$

is the kernel of the transformation (filtering-photodetection-filtering). As $K^*(v, u) = K(u, v)$ the kernel is symmetric. Furthermore, since the kernel is continuous, it can be expanded into a series using orthogonal functions

$$K(u, v) = \sum_{i=1}^{\infty} \frac{\Phi_i(u)\Phi_i^*(v)}{\lambda_i} \tag{6}$$

where λ_i and $\Phi_i(x)$ are the eigenvalues and eigenfunctions satisfying the following equation

$$\Phi_i(x) = \lambda_i \int_{-\infty}^{\infty} K(x, y)\Phi_i(y)dy, \; x \in \{u, v\}. \tag{7}$$

Note that we use the inverse kernel definition for relation (6) [6]. Substituting (6) into (4) the electrical filter output becomes

$$I(t) = \sum_{i=1}^{\infty} \frac{|s_i(t) + n_i(t)|^2}{\lambda_i}, \tag{8}$$

where

$$s_i(t) = \int_{-\infty}^{\infty} s(t-\tau)\Phi_i(\tau)d\tau$$
$$n_i(t) = \int_{-\infty}^{\infty} n(t-\tau)\Phi_i(\tau)d\tau. \tag{9}$$

A set of the orthonormalized functions is chosen in such a way that the coefficients n_i are uncorrelated [6], i.e., $m_1(n_i^2) = R_n(0)$, with m_1 being the first-order moment of the noise process [6].

Following the similar procedure described in [3–4], [6], we can write the characteristic function of the electrical filter output signal as follows

$$C_I(j\Omega) = \prod_{i=1}^{\infty} \frac{1}{1 - (2j\Omega R_n(0)/\lambda_i)} \exp\left[\frac{|s_i|^2}{2R_n(0)} \frac{2j\Omega R_n(0)}{\lambda_i - 2j\Omega R_n(0)}\right]. \tag{10}$$

The natural logarithm of the characteristic function can be expanded using Taylor series formula

$$\ln[C_I(j\Omega)] = \sum_{n=1}^{\infty} \frac{\kappa_n}{n!}(j\Omega)^n, \tag{11}$$

where the coefficients in the expansion are

$$\kappa_n(t) = (-j)^n \frac{d^n}{d\Omega^n} \ln[C_I(j\Omega)]|_{\Omega=0} = (2R_n(0))^n n! \cdot \left[\frac{1}{R_n(0)} \int_{-\infty}^{\infty} \int_{-\infty}^{\infty} s(t-u) K^{(n)}(u,v) s^*(t-v) du dv + \frac{1}{n} \int_{-\infty}^{\infty} K^{(n)}(u,u) du \right] \quad (12)$$

$K^{(n)}(u, v)$ is the n^{th} order kernel, defined iteratively:

$$K^{(n)}(u,v) = \int_{-\infty}^{\infty} K^{(n-1)}(u,w) K(w,v) dw, \; n \geq 2$$
$$K^{(1)}(u,v) \equiv K(u,v) \quad (13)$$

Finally, the probability density function of decision statistics $w(x)$ can be found using the following definition expression

$$w(x) = \frac{1}{2\pi} \int_{-\infty}^{\infty} C_I(j\Omega) \exp[-j\Omega x] d\Omega \quad (14)$$

Although the derivation of the model is certainly not straightforward, it is conceptually very simple. The difficulties arise only in numerical calculations of the expansion coefficients (12). To calculate the probability density function from the characteristic function (14) the efficient FFT algorithm may be applied. If the optical filter is modeled as a super-Gaussian filter, and electrical filter modeled as a Gaussian filter, and NRZ signals are observed, the coefficient of Taylor expansion can be determined in a closed form

$$\kappa_n \approx \frac{(2bR_n(0)B_1)^n (n-1)!}{\left(\sqrt{b^2+2}+b\right)^n - \left(\sqrt{b^2+2}-b\right)^n} \left[1 + \frac{0.5P_{av}}{R_n(0)B_1} \sqrt{\frac{\left(\sqrt{b^2+2}+b\right)^n - \left(\sqrt{b^2+2}-b\right)^n}{\left(\sqrt{b^2+2}+b\right)^n + \left(\sqrt{b^2+2}-b\right)^n} \frac{\sqrt{b^2+2}}{b}} \right], \quad (15)$$

where B_1 is the equivalent optical filter bandwidth

$$B_1 = \int_{-\infty}^{\infty} |H_1(j\omega)|^2 d\omega \quad (16)$$

with $H_1(j\omega)$ being the optical filter transfer function. $b = 2B_2/B_1$, where B_2 is the equivalent electrical filter bandwidth

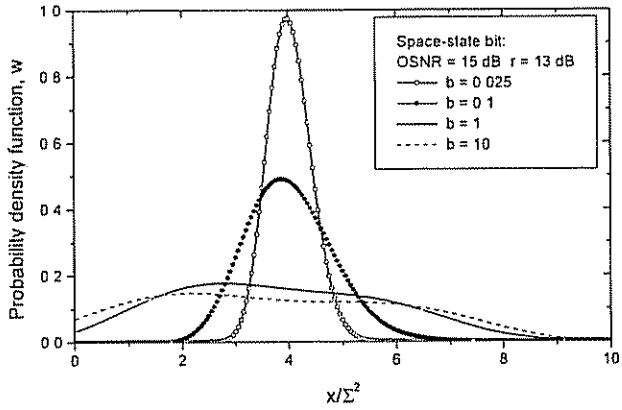

Fig. 2. Probability density function of decision statistics for a space state bit

$$B_2 = \int_0^{\infty} |H_2(j\omega)|^2 d\omega, \quad (17)$$

with $H_2(j\omega)$ being the electrical filter transfer function. (Pav is the observed bit average optical power).

2.2 Numerical Results and Discussion

To illustrate the proposed model, a PDF of the decision circuit input noise for a space-state bit is shown in Figure 2.

The curves in Figure 2 are obtained under the assumption that the optical filter is modeled as a super-Gaussian filter, that the electrical filter is modeled as Gaussian and that the signal is NRZ. It is evident that for a space-state bit, the PDF curve is like Gaussian just as in the case when the ratio b is close to zero. To assess the validity of Gaussian approximation of decision statistics, we define, similarly as in [7–8], the skewness (asymmetry coefficient) α and the kurtosis (flatness coefficient) β respectively:

$$\alpha = m_3 \Big/ \sqrt{M_2^3} \text{ and } \beta = M_4/M_2^2 - 3, \quad (18)$$

where M_n is the central moment of the n^{th} order [6]. The skewness describes the symmetry ($\alpha = 0$) or asymmetry ($\alpha \neq 0$) of PDF curve with respect to the center mass axis, while the kurtosis describes whether the PDF curve is more narrow with higher peak ($\beta > 0$) than Gaussian distribution ($\beta = 0$) or vice versa ($\beta < 0$). The skewness and the kurtosis coefficients versus optical signal-to-noise ratio (OSNR, defined in B_1 bandwidth) are shown in Figures 3–4.

For the mark-state bit and OSNR greater than 20 dB the flatness coefficient is close to zero for any electrical-filter bandwidth-to-optical filter bandwidth ratio (b), while

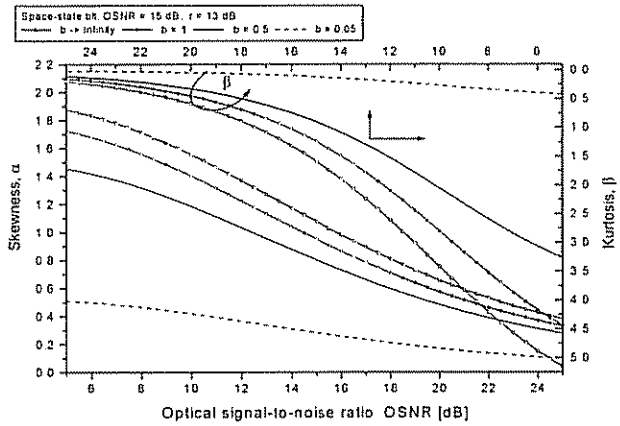

Fig. 3. The skewness and the kurtosis for a space-state bit.

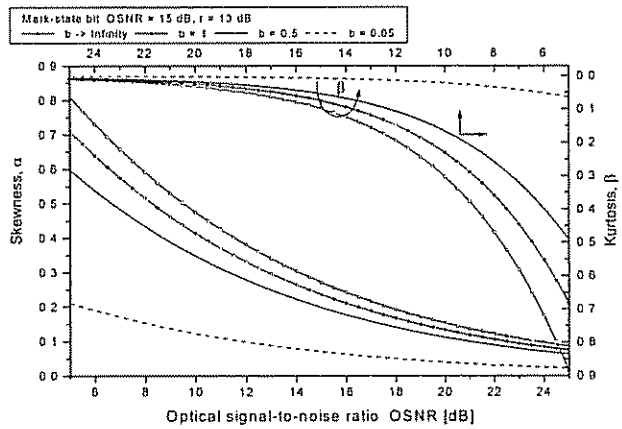

Fig. 4. The skewness and the kurtosis for a mark-state bit.

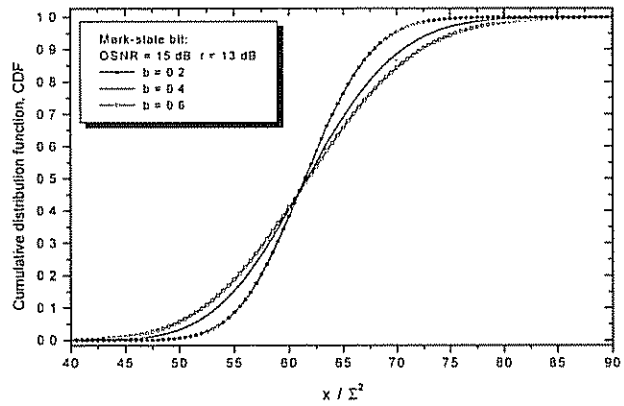

Fig. 5. Cumulative distribution function for a mark-state bit.

the coefficient of asymmetry tends to zero only when b converges to zero. For the space-state bit the PDF is always different from Gaussian. Strictly speaking the decision statistics is never Gaussian.

For a typical the electrical filter bandwidth of 0.65 R_b (R_b is the bit rate) and optical filter bandwidth region ($2R_b$, $5R_b$) the ratio $2B_2/B_1$ is in an interval (0.26, 0.6) and the decision statistics is far from Gaussian. The cumulative distribution function for a mark-state bit for different values of ratio b is shown in Figure 5, while the bit-error rate is shown in Figure 6.

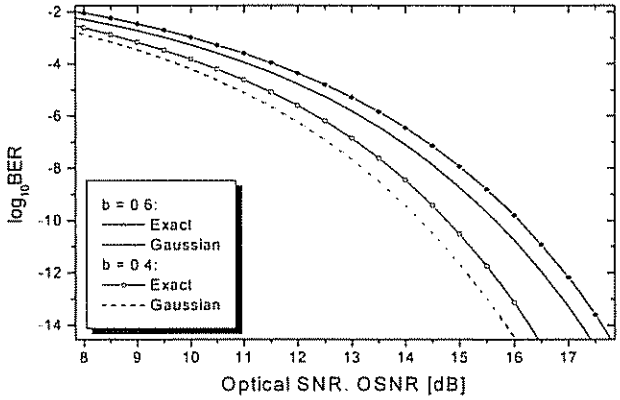

Fig. 6. Bit-error rate vs. optical signal-to-noise ratio.

For the bit-error rate (BER) of 10^{-12} and a typical value of ratio $b = 0.6$ the approximation error obtained when the exact PDF is approximated by Gaussian with the mean value and the standard deviation determined from exact PDF is 0.45 dB.

3. Direct detection receiver modeling

3.1 Receiver model description

The optical filter output noise is a zero-mean process with an autocorrelation function

$$R_N(\tau) = \int_{-\infty}^{\infty} R_{h_1}(t) R_n(\tau - t) dt, \tag{19}$$

where $R_{h_1}(\tau)$ is the autocorrelation function of the optical filter impulse response

$$R_{h_1}(\tau) = \int_{-\infty}^{\infty} h_1(t) h_1^*(t+\tau) d\tau, \tag{20}$$

where the asterisk (*) denotes complex conjugate. (Notation is the same as that used in Section 2). The PIN photodiode output can be written as

$$\begin{aligned} i(t) &= R|S(t) + N(t)|^2 \\ &= R[|S(t)|^2 + |N(t)|^2 + 2R_e\{S(t)N^*(t)\}], \end{aligned} \tag{21}$$

R is the photodiode responsivity and will be omitted in further derivations without loss of generality and R_e denotes the real part of a complex number.

The electrical filter output $I(t)$ is the convolution of the photodiode current $i(t)$ and the electrical filter impulse response $h_2(t)$

$$I(t) = \int_{-\infty}^{\infty} h_2(\tau) i(t-\tau) d\tau. \tag{22}$$

The electrical filter output signal mean follows

$$\overline{I(t)} = \int_{-\infty}^{\infty} |S(\tau)|^2 h_2(t-\tau) d\tau + R_N(0), \tag{23}$$

where the overbar denotes the ensemble averaging. In deriving the Equation (23), the following normalization was used

$$\int_{-\infty}^{\infty} h_2(t) dt = H_2(0) = 1. \tag{24}$$

By using (24), the electrical filter output signal autocorrelation function can be written as

$$\begin{aligned} R_I(t_1, t_2) = & \int_{-\infty}^{\infty} |S(\tau)|^2 h_2(t_1-\tau) d\tau \cdot \\ & \int_{-\infty}^{\infty} |S(\tilde{\tau})|^2 h_2(t_2-\tilde{\tau}) d\tilde{\tau} + R_N^2(0) + \\ & R_N(0) \int_{-\infty}^{\infty} |S(\tau)|^2 h_2(t_1-\tau) d\tau + \\ & R_N(0) \int_{-\infty}^{\infty} |S(\tilde{\tau})|^2 h_2(t_2-\tilde{\tau}) d\tilde{\tau} + \\ & 2R_e \left\{ \int_{-\infty}^{\infty} \int_{-\infty}^{\infty} S(\tau) S^*(\tilde{\tau}) R_N(\tau-\tilde{\tau}) \cdot \right. \\ & \left. h_2(t_1-\tau) h_2(t_2-\tilde{\tau}) d\tau d\tilde{\tau} \right\} + \\ & 2 \int_{-\infty}^{\infty} \int_{-\infty}^{\infty} h_2(t_1-\tau) |R_N(\tau-\tilde{\tau})|^2 h_2(t_2-\tilde{\tau}) d\tau d\tilde{\tau}. \end{aligned} \tag{25}$$

The first four terms are DC terms, the fifth one is the signal-noise beating term in the photodiode, and the last term comes from noise-noise beating. Note that the mean and the autocorrelation are now functions of time, which means that the electrical filter output process is not stationary. The reason is that the photodiode is a non-linear element regarding the electrical field.

Starting from the expression for the autocovariance

$$L_I(t_1, t_2) = R_I(t_1, t_2) - \overline{I(t_1)} \cdot \overline{I(t_2)}. \tag{26}$$

the variance can be determined by putting $t_1 = t_2 = t$. The derivation of the expression for the variance of the process at the output of an electrical filter is then straightforward, and after inserting the shot noise term $q\overline{I(t)}$, q being electron charge, and the electronic circuitry term σ_{elec}^2, which include both transmitter and receiver electronic noise, also known as "back-to-back" noise, we obtain

$$\begin{aligned} \sigma^2(t) = & 2R_e \left\{ \int_{-\infty}^{\infty} \int_{-\infty}^{\infty} S(\tau) S^*(\tilde{\tau}) R_N(\tau-\tilde{\tau}) \cdot \right. \\ & \left. h_2(t-\tau) h_2(t-\tilde{\tau}) d\tau d\tilde{\tau} \right\} + \\ & 2 \int_{-\infty}^{\infty} \int_{-\infty}^{\infty} h_2(t-\tau) |R_N(\tau-\tilde{\tau})|^2 h_2(t-\tau) d\tau d\tilde{\tau} + \\ & q\overline{I(t)} + \sigma_{elec}^2. \end{aligned} \tag{27}$$

If there is no polarization filter the second term in (27) should be multiplied by a factor 2. Bit error probability can be calculated using the Gaussian approximation [2], [10] at the sample time

$$P_e = \frac{1}{N_b} \sum_{n=0}^{N_b-1} \frac{1}{2} erfc\left(\frac{|I(n) - I_{tsh}|}{\sigma(n)\sqrt{2}} \right), \tag{28}$$

where N_b is the PN generator length. The length of a PN generator is to be long enough long so that all possible combinations, that cause ISI, occur at least once. With $I(n)$ and $\sigma(n)$ as the mean and standard deviation of the n^{th} bit samples determined using the expressions (23) and (27), I_{tsh} as the decision threshold, the error function is defined as

$$erfc(x) = \frac{2}{\sqrt{\pi}} \int_{x}^{+\infty} e^{-u^2} du. \tag{29}$$

Although the Gaussian approximation is applied at the sample time its parameters (the mean and the standard deviation) are functions of time (see expressions (23) and (27)) and resulting process is not even more stationary, let alone Gaussian. We show later in the text, that such an approach gives an excellent agreement with

Monte Carlo simulations. Alternatively, the exact expression for probability density function, described in Section 2, may be used in the bit-error rate calculation.

3.2 Numerical results and discussion

The results of calculation for different modulation schemes, namely NRZ, RZ, CRZ and CSRZ are shown in Figures 7–9. The optical filter is modeled as super Gaussian of order eight, while the electrical filter is modeled as Gaussian. No FEC is applied and no fiber nonlinearities are considered, although the model is general and independent on pulse shape. It is confirmed that the optimum electrical filter bandwidth exists. Results are obtained for optimally chosen threshold, and omitting the polarization filter.

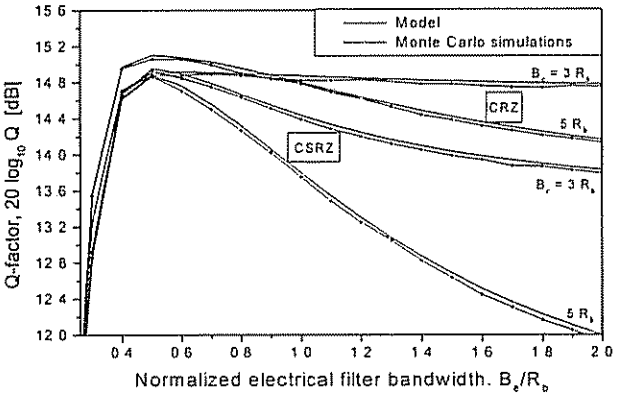

Fig. 7. Proposed receiver model vs. Monte Carlo simulation for two typical modulation schemes for long-haul communications (CRZ with modulation depth 1 and phase modulation index 1 rad and CSRZ) and two different optical filter bandwidths ($5R_b$ and $3R_b$). Bit rate is 10 Gb/s, extinction ratio 13 dB, Q-factor in absence of ASE noise (determined by transmitter and receiver electronics) is 23 dB. Optical signal-to-noise ratio is 15 dB

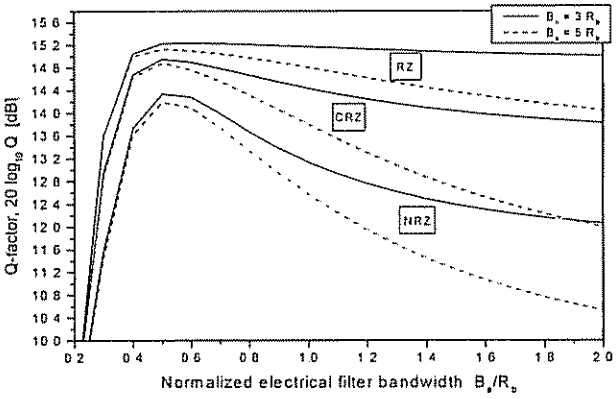

Fig. 8. Comparison among different modulation schemes (NRZ, RZ with duty cycle 0.33, CSRZ) using the proposed receiver model. The set of parameters is the same as in Figure 5.

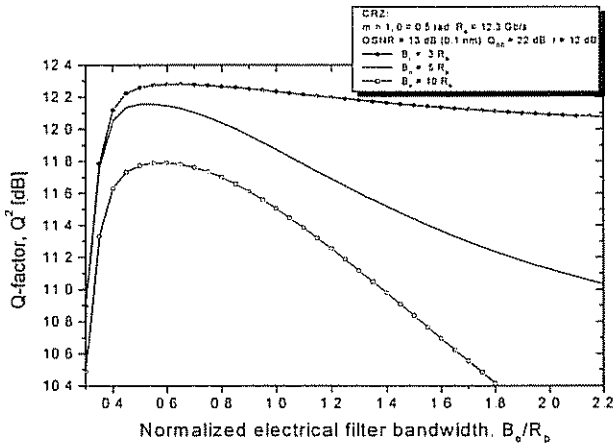

Fig. 9. Q-factor in the absence of MPI vs. electrical filter bandwidth for CRZ with a phase modulation index of 0.5 rad.

The Q-factor is determined starting from expression (28) by

$$P_e = \frac{1}{2} erfc\left(\frac{Q}{\sqrt{2}}\right). \tag{30}$$

The Q-factor variation with electrical filter bandwidth B_e, normalized with bit rate R_b, for two different modulation schemes, CRZ and CSRZ, and two different optical filter bandwidths $B_o = 5R_b$ and $B_o = 3R_b$ is shown in Figure 7.

Curves obtained using the proposed method (full lines) and Monte Carlo simulations ('diamond' marked curves) show excellent agreement. The figure also illustrates as to which modulation scheme is better. For the region of electrical filter bandwidth ($0.4R_b$, $0.65R_b$), the CSRZ for both optical filter bandwidths is found to give comparable results to that of CRZ for optical filter bandwidth of $3R_b$ with amplitude modulation depth 1 and phase modulation index 1 rad. Nevertheless, CRZ is least sensitive to the choice of any electrical filter bandwidth. Moreover, for this particular optical filter bandwidth the electrical filter can be omitted without much degradation in performance. CRZ with optical filter bandwidth $5R_b$ is found to be always better.

Figure 8 allows for making comparison among different modulation schemes.

It is observed that CSRZ is always better than NRZ, while RZ with duty cycle 0.33 is always better than NRZ and CSRZ. RZ (CRZ with phase modulation index 0 rad) is observed to give the best performance. In Figure 9 are shown the results for the most popular modulation format in long-haul communications, chirped-return-to-zero (see [1] for CRZ description).

Long-haul transmission with the line rate 12.3 Gb/s is observed. (The 10 Gb/s system employing RS(255,239) +RS(255,223) FEC scheme has the same bit rate). For large phase modulation indices and small optical filter bandwidths, CRZ is found to be less sensitive to the

choice of electrical filter bandwidth. But, if the optical filter bandwidth becomes too small electrical filter efficiency decreases.

4. Multi-path interference modeling

4.1 MPI model description

The electrical field of an observed channel at the optical filter input for n^{th} bit slot can be written as

$$E_n(t) = \sum_{k=-\infty}^{\infty} E_{n,k}(t - cT - (n-1)T + kT), \qquad (31)$$

where the slot n of electrical field in the presence of ISI coming from k^{th} time slot can be written in the form of Jones vector as

$$E_{n,k}(t) = \begin{bmatrix} E_{x.n.k}(t) \\ E_{y.n.k}(t) \end{bmatrix} = \begin{bmatrix} \sqrt{d_{n+k}(1-p)P}\, g_{n+k}(t) + N_x^{ASE}(t) + N_x^{MPI}(t) \\ \sqrt{d_{n+k}pP}\, g_{n+k}(t) e^{j\Phi} + N_y^{ASE}(t) + N_y^{MPI}(t) \end{bmatrix}, \qquad (32)$$

where: $N_x^{\text{ASE}}(t)$ and $N_x^{\text{MPI}}(t)$ are the complex representations of ASE noise and MPI, respectively; having the same state of polarization as the observed channel signal. N_y^{ASE} and N_y^{MPI} are the noise components of ASE and MPI, respectively; orthogonal to the signal state of polarization. P is the peak power per channel, $d_n \in \{r, 1\}$, $0 < r < 1$ is the information content (r-the extinction ratio). $g_n(t)$ is the n^{th} bit pulse shape that could vary from bit to bit depending on the fiber nonlinearities and dispersion, and modulation statistics as well. Both ASE noise components and the MPI components are considered to be colored Gaussian. The power spectral density of ASE noise is determined by the EDFA output filter, while that of MPI by the signal spectrum. To determine the spectrum of MPI the spectrum of an isolated pulse was observed, properly normalized so that its power be equal to the average MPI power, and each spectral component was uniformly randomized in phase. The state of polarization is described by power splitting ratio p ($0 \le p \le 1$) and phase difference Φ between y- and x-polarization components. Centering factor c takes a pulse position with respect to bit frame into account, T is the bit duration. The summation (31) takes into account the influence of the neighboring bits, that is ISI.

4.2 Q-factor Degradation due to MPI

The system penalty coming from MPI was estimated in [5], [17–21] using the Gaussian Crosstalk model. This model assumes that the signal-MPI beating dominates MPI-MPI beating. Starting from [20] the power penalty, defined as increase in received optical power in the presence of MPI (P_s') to have the same Q-factor as in the absence of MPI (P_s) follows

$$-10\log_{10}\frac{P_s}{P_s'} = -10\log_{10}\frac{2}{1+\sqrt{1+2Q^2\epsilon}}, \qquad (33)$$

with ϵ being the MPI crosstalk level. Under assumption that $\epsilon \ll 1/(2Q^2)$ and applying the Taylor expansion the well-known expression for power penalty follows

$$-10\log_{10}\frac{P_s}{P_s'} = -10\log_{10}\left(1 - \frac{1}{2}Q^2\epsilon\right). \qquad (34)$$

Due to the fact that the light is scattered randomly in all directions and that it could appear at any point during transmission in long-haul link, and that different MPI sources are uncorrelated with different phases we assume that MPI signal is an average of mark- and space-state bits from direct signal and it is depolarized. We further assume that MPI is a stationary process with a non-flat power spectral density determined by the signal spectrum. The performance degradation coming from MPI, defined as the ratio in Q-factor in the presence Q and absence of MPI Q_0,

$$\Delta Q = -20\log_{10}\frac{Q}{Q_0}[\text{dB}], \qquad (35)$$

is illustrated in Figures 10–12 for CRZ with line rate 12.3 Gb/s (the extinction ratio is set to 12 dB, 'back-to-back' Q-factor (in the absence of ASE and MPI) is 23 dB). Results shown in Figure 10 corresponds to the hybrid Raman/EDFA chain, while those in Figure 11 to all-Raman based systems.

That all-Raman based systems are much more sensitive on MPI than hybrid amplifiers can be concluded from given figures. Also, the greater the phase modulation index is, the smaller Q-factor degradation due to MPI is, Figure 12 suggests.

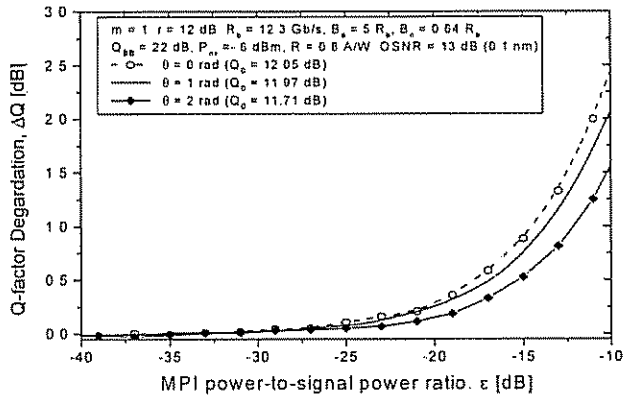

Fig. 10. Q-factor degradation due to MPI for CRZ with different phase modulation indexes for OSNR = 13 dB in 0.1 nm.

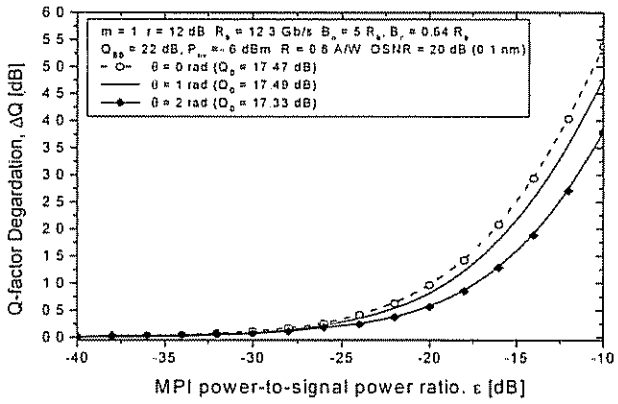

Fig. 11. Q-factor degradation due to MPI for CRZ with different phase modulation indexes for OSNR = 20 dB in 0.1 nm

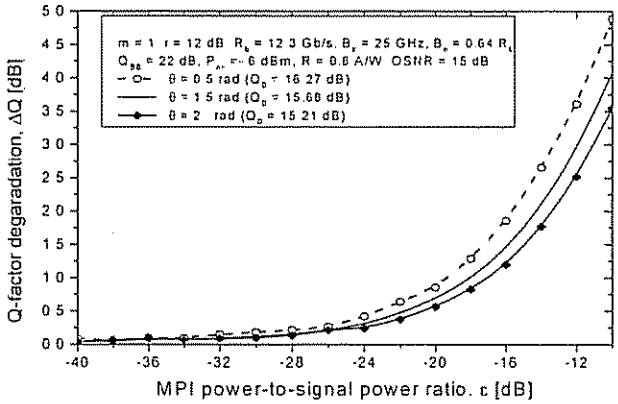

Fig. 12. Q-factor degradation due to MPI for CRZ and different values of phase modulation index

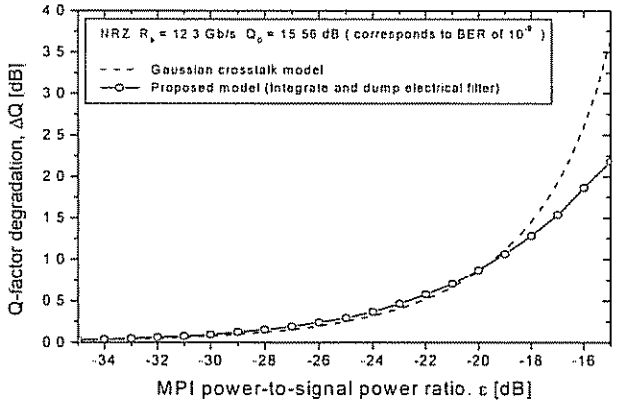

Fig. 13. Comparison of proposed MPI and Gaussian crosstalk model

The comparison between the proposed model and Gaussian crosstalk model is shown in Figure 13, for Q-factor being set to 15.56 dB (bit-error rate is then 10^{-9}).

Previously reported Gaussian crosstalk model gives reasonable results when the crosstalk coming from MPI is less than −20 dB. For greater crosstalk levels Gaussian crosstalk model overestimates the degradation coming from MPI.

5. Conclusion

An advanced method to determine the exact decision statistics of direct detection receiver is proposed in this paper. It is independent on the choice of optical and electrical filters and independent on the modulation scheme. The additive noise (ASE, MPI, etc.) is modeled as a stationary noise with an autocorrelation function that is obtained experimentally. The comparison with the Gaussian approximation of decision statistics is given and its in-applicability in practice is pointed out. A novel receiver model independent on the modulation format, pulse shape, electrical and optical filter choice is proposed. This model includes ISI, ASE noise, MPI for long-haul communications and other type of noises that can be modeled as stationary processes. The model is compared against Monte Carlo simulations and perfect agreement is found. The proposed receiver model is applied to compare different modulation schemes (NRZ, RZ, CRZ and CSRZ). RZ (CRZ with phase modulation index 0 rad) is observed to give the best performance. For large phase modulation indices and small optical filter bandwidths, CRZ is found to be less sensitive to the choice of electrical filter bandwidth. But, if the optical filter bandwidth becomes too small electrical filter efficiency decreases. A novel MPI model independent on MPI crosstalk level, modulation format, optical and electrical filter choice is also proposed in this paper. The components of MPI are considered independent of each other and depolarized with the power spectral density determined by the signal spectrum. The comparison with widely used Gaussian crosstalk model is made and limits of its application are pointed out.

Acknowledgement. The authors acknowledge technical assistance of Dr. Saša V. Djordjevic and Dr. G. B. Ren.

References

[1] Golovchenko, E. A.; Pilipetskii, A. N.; Bergano, N. S.; Davidson, C. R.; Khatri, F. I.; Kimball, R. M.; Mazurczuk, V. J.: Modeling of Transoceanic Fiber-Optic WDM Communication systems. IEEE Journal of Selected Topics in Quantum Electronics **6**(2) (March/April 2000), 337–347.

[2] Winzer, P. J.; Pfennigbauer, M.; Strasser, M. M.; Leeb, W. R.: Optimum Filter Bandwidths for Optically Preamplified NRZ Receivers. Journal of Lightwave Technology **19**(9) (2001), 1263–1273.

[3] Monroy, I. T.: On analytical expressions for the distribution of the filtered output of square envelope receivers with signal and colored gaussian noise input. IEEE Transactions on Communications **49**(1) (2001), 19–23.

[4] Bosco, G.; Carena, A.; Curri, V.; Gaudino, R.; Poggiolini, P.; Benedetto, S.: A novel analytical method for the BER evaluation in optical systems affected by parametric Gain. IEEE Photonics Technology Letters **12**(2) (2000), 152–154.
[5] Fludger, C. R. S.; Mears, R. J.: Electrical Measurements of Multhipath Interference in Distributed Raman Amplifiers. Journal of Lightwave Technology **19**(4) (2001), 536–545.
[6] McDonough, R. N.; Whalen, A. D.: Detection of Signals in Noise. Academic Press-San Diego-USA, Second Edition, 1995.
[7] Levin, B. R.: Statistical Radio Communication Theory Basics I, Sovetskoe Radio: Moscow-Russia, 1974. (in Russian).
[8] Press, W. H.; Teukolsky, S. A.; Vetterling, W. T.; Flannery, B. P.: Numerical Recipes in C. Cambridge University Press: Cambridge-New York-Port Chester-Melbourne-Sydney 1997.
[9] Humblett, P. A.; Azizoglu, M.: On the Bit Error Rate of Lightwave Systems with Optical Amplifiers. Journal of Lightwave Technology **9**(11) (1991), 1576–1582.
[10] Pauer, M.; Winzer, P. A.: Bit Error Probability Reduction in Direct Detection Optical Receivers Using RZ Coding. Journal of Lightwave Technology **19**(9) (2001), 1255–1262.
[11] Jacobsen, G.; Berlitzon, K.; Xiapin, Z.: WDM Transmission System Performance: Influence of non-Gaussian Detected ASE Noise and Periodic DEMUX Characteristic. Journal of Lightwave Technology **16**(10) (1998), 1804–1812.
[12] Monroy, I. T.: Bit Error Evaluation of Optically Preamplified Direct Detection Receivers with Fabry-Perot Optical Filters. Journal of Lightwave Technology **15**(8) (1997), 1546–1553.
[13] Saito, S.; Matsuda, T.; Naka, A.: Optical Amplifiers and Their Applications '97. Paper TuD11-1, Victoria, BC, 1997.
[14] Boivin, L.; Pendock, G. J.: Receiver Sensitivity for Optically amplified RZ signal with Arbitrary Duty cycle. Optical Amplifiers and Their Applications '99, paper ThB4, pp. 106–109, 1999.
[15] Grosz, D. F.; Kung, A.; Maywar, D. N.; Altman, L.; Movassaghi, M.; Lin, H. C.; Fishman, D. A.; Wood, T. H.: Demostration of All-Raman Ultra-Wide-Band Transmission of 1.28 Tb/s (128 × 10 Gb/s) over 4000 km NZ-DSF with Larg BER Margins. 27th European Conference on Optical Communication (ECOC'01)-Proceedings-Volume 6, pp. 72–73, 2001.
[16] Carena, A.; Curri, V.; Poggiolini, P.: On the Optimization of Hybrid Raman/Erbium-Doped Fiber Amplifiers. IEEE Photonics Technology Letters **13**(11) (2001), 1170–1172.
[17] Eskildsen, L.; Hansen, P. B.: Interferometric Noise in Lightwave systems with Optical Preamplifiers. IEEE Photonics Technology Letters **9**(11) (1997), 1538–1540.
[18] Nissov, M.; Rotwitt, K.; Kidorf, H. D.; Ma, M. X.: Rayleigh Crosstalk in Long Cascades of Distributted Unsaturated Raman Amplifiers. Electronics Letters **35**(12) (1999), 997–998.
[19] Hansen, P. B.; Eskildsen, L.; Stenz, A. J.; Strasser, T. A.; Judkins, J.; DeMarco, J. J.; Pedrazzani, R.; DiGiovanni, D. J.: Rayleigh scattering Limitations in Distributed Raman Pre-Amplifiers. IEEE Photonics Technology Letters **10**(1) (1998), 159–161.
[20] Wan, P.; Conradi, J.: Impact of Double Rayleigh Backscatter Noise on Digital and Analog Fiber Systems. Journal of Lightwave Technology **14**(3) (1996), 288–297.
[21] Yadlowsky, M. J.; da Silva, V. L.: Experimental Comparison of the Effect of Discrete and Distributed Path Inband Crosstalk on System Performance: Application to Predicting System Performance Penalties. Journal of Lightwave Technology **16**(10) (1998), 1813–1821.

Ivan B. Djordjevic received his B.Sc., M.Sc., and Ph.D. degrees in electrical engineering from the Faculty of Electronic Engineering, University of Nish, Nish, Serbia and Montenegro, in 1994, 1997, and 1999, respectively. From 1994 to 1996 he was with the Faculty of Electronic Engineering, University of Nish, working on modelling and simulation of optical/digital communication systems. He was involved in digital transmission systems commissioning and acceptance, design, maintenance, installation, and connection from 1996 to 2000, when he was with the State Telecommunications Company, District Office for Networks, Nish, Serbia. From 2000 to 2001 he was a Postdoctoral Fellow with the National Technical University of Athens, Greece, working on fibre nonlinearities and MAN and WAN modelling and simulation. Then, in the second half of 2001, he was with TyCom US Inc., USA, where he was involved in receiver modelling for DWMD systems. During 2002 he was with the University of Arizona, USA, working on low-density parity check codes and iterative decoding for long-haul transmission as well as on simulation and modelling of DWDM systems. He is now with the University of Bristol, UK. Dr. Djordjevic is the author of more than 60 publications in international journals and conference proceedings. His research interests include DWDM fibre-optic communication systems and networks, coding for optical communications, coherent optical communications, information theory, and statistical communication theory.

Bane V. Vasic received his B.Sc., M.Sc., and Ph.D., all in electrical engineering, from the University of Nish, Serbia. From 1996 to 1997 he worked as a Visiting Scientist at the Rochester Institute of Technology and Kodak Research, Rochester, NY, where he was involved in research in optical storage channels. From 1998 to 2000 he was with Lucent Technologies, Bell Laboratories. He was involved in research in read channel architectures and iterative decoding and low-density parity check codes, as well as development of codes and detectors for five generations of Lucent (now Agere) read channel chips. Presently, Dr. Vasic is a Faculty Member of the University of Arizona, Electrical and Computer Engineering Department. He has authored more than 15 journal articles and more than 50 conference articles. He is a Member of the Editorial Board of the IEEE Transactions on Magnetics. He serves as a Technical Program Chair, IEEE Communication Theory Workshop, 2003, and as Co-organizer of the Center for Discrete Mathematics and Theoretical Computer Science (DIMACS) Workshop on Optical/Magnetic Recording and Optical Transmission, 2003. His research interests include coding theory, information theory, communication theory, and digital communications and recording.